Article:
Manning, J.R.H., Walkley, B., Provis, J.L. et al. (1 more author) (2021) Mimicking bio-sintering: the identification of highly condensed surfaces in bioinspired silica materials. Langmuir, 37 (1). pp. 561-568. ISSN 0743-7463

https://doi.org/10.1021/acs.langmuir.0c03261

Mimicking bio-sintering: The identification of highly condensed surfaces in bioinspired silica materials

Joseph RH Manning[1,2,3], Brant Walkley[1,4], John L. Provis[4] and Siddharth V. Patwardhan[1]*

[1] *Department of Chemical and Biological Engineering, The University of Sheffield, Sheffield S1 3JD, UK.*
[2] *Department of Chemical Engineering, The University of Bath BA2 7AY, UK,*
[3] *Department of Chemistry, University College London, WC1E 6BT, UK*
[4] *Department of Materials Science and Engineering, The University of Sheffield, Sheffield S1 3JD, UK.*
**s.patwardhan@sheffield.ac.uk*

ORCiD IDs. JM: 0000-0002-3755-5902, BW: 0000-0003-1069-1362, JP: 0000-0003-3372-8922, SP: 0000-0002-4958-8840

Abstract

Interfacial interactions between inorganic surfaces and organic additives are vital to develop new complex nanomaterials. Learning from biosilica materials, composite nanostructures have been developed, which exploit the strength and directionality of specific polyamine additive-silica surface interactions. Previous interpretations of these interactions are almost universally based on interfacial charge matching and/or hydrogen bonding. In this study we analysed the surface chemistry of bioinspired silica (BIS) materials using solid-state nuclear magnetic resonance (NMR) spectroscopy, as a function of organic additive concentration. We found significant additional association between the additives and fully condensed (Q^4) silicon species compared to industrial silica materials, leading to more overall Q^4 concentration and higher hydrothermal stability despite BIS having a shorter synthesis time. We posit the polyfunctionality and catalytic activity of additives in the BIS synthesis leads to both these surface phenomena, contrasting previous studies on monofunctional surfactants used in most other artificial templated silica syntheses. From this, we propose that additive polyfunctionality can be used to generate tailored artificial surfaces *in situ* and provide insight into the process of bio-sintering in biosilica systems, highlighting the need for more in-depth simulations on interfacial interactions at silica surfaces.

Introduction

Understanding the interactions of small organic molecules with inorganic surfaces is key to controlling the formation and behaviour of both biological and artificial nanomaterials. Protein-mediated synthesis of nanomaterials with specific shape and function is common in nature, creating nanomaterials such as hydroxyapatite in bone,[1] biosilica as spicules in sponges and frustules in diatoms,[2,3] and magnetite crystals in some bacteria.[4] *In vitro*, the activity of these biomolecules has been widely studied for material synthesis, leading to the biomimetic synthesis of inorganic chalcogenides,[5] metals,[6,7] and even carbon nanotubes,[8] with the structural properties of each determined by the specific interaction between the biomolecule and inorganic constituents.

In order to take advantage of these interactions, the use of organic additives or templates have been studied extensively for several fully artificial or biologically inspired templated material systems. Taking the case of amorphous silica (a technologically important material with US$4 billion per annum market),[9] surfactant molecules have been widely investigated to direct long-range, ordered porosity in the materials.[10,11] Separately, combining the mild and sustainable synthesis conditions of natural silica with the scalability of industrial silica,[12] 'bioinspired silica' (BIS) materials have been synthesised using a variety of small molecules or polymers with biomolecule-like moieties to direct their growth.[13–15]

Given the central role of interfacial processes in structure direction, surface interactions have been studied widely, usually using either solid-state magic angle spinning (MAS) nuclear magnetic resonance (NMR) spectroscopy[16–18] or molecular dynamics simulations.[19–21] For artificial silicas i.e. surfactant templated MCM-41 and related materials, NMR is useful to elucidate the specific organic-silica binding in solution that leads to different surface chemistry from acidic or basic pathways.[22] Further, NMR has also been used to study the chemistry of surfactant templates without permanent charges to detect the nature of template-silica interactions during synthesis.[23,24] Similarly, for BIS and biomimetic silica materials, there have been previous investigations into how the chemistry of the additive (charged vs uncharged) affect both polymerisation and solid silica condensation degree.[25–27]

In biosilica materials, however, investigation into interfacial interactions has long been hampered by the low natural abundance of NMR active ^{29}Si, ^{13}C, and ^{15}N in the inorganic and organic phases, respectively.[28] Accordingly, several studies have focussed on analysing the organic phase themselves to determine the impact of confinement within a silica matrix.[29,30] To overcome this limitation, several researchers have studied isotopic labelling of the biomolecules,[31] and of diatoms themselves,[28] enabling more direct investigations of biosilica materials. Similarly, proxy studies have been carried out using organic compounds like isotopically-labelled choline[26] or single amino acids[32] adsorbed onto artificial silicas, and signal amplification using Dynamic Nuclear Polarisation[33] or REDOR[28] NMR in conjunction with biomolecules to probe chemistry at the interface.

In the case of BIS, use of amine-based polymers as additives rather than neutral tertiary amine-based counterparts (or no organic component at all) was found to both promote synthesis of silica and lead to a more highly condensed material.[25] This "extra" polymerisation was attributed to the established catalytic effect of polyamines on silica polymerisation,[13] signifying that bioinspired additives catalyse both the early stages of silica growth but also its deposition into larger agglomerates. In artificial templated silicas, ^{1}H-^{29}Si Cross Polarisation (CP) MAS NMR, where ^{29}Si signals were amplified according to the proximity of protons, has enabled more in-depth studies, identifying different template-silanol interactions for samples produced at high and low pH values.[22]

Similar phenomena have been shown during analysis of biomolecule-silicas systems as a function of adsorbed water.[26,34] In these studies, biomolecule-surface hydrogen bonding was only abundant at solvated surfaces, whereas charge-matching ammonia-silica interactions were highly prevalent in fully dry materials. This agrees with simulations of fully solvated silicas too, where the nature of bonding has been shown to be a function of surface ionisation, hence pH.[19,35] Few classical simulation studies indicated there would be significant hydrogen bonding between biomolecules and fully condensed siloxane bonds. One notable case is the simulated adsorption of ammonium-based surfactants onto clay materials with no exposed silanol functionality;[36,37] hydrogen bonding of ammonium headgroups into Q^4 clusters was detected, indicating an interaction strength of up to 50 kJ/mol.[37] Despite these predictions, no equivalent interactions have been detected on surfaces containing free silanol and

siloxane Q^3 species, presumably due to the increased strength of charge-matching interactions (ca. 250 kJ/mol).[35] Conversely, ab initio simulations[34] and NMR investigations of isotopically enriched biological silicas[28] have identified the possibility of a biomolecule-siloxane silica interaction.

However, experimental studies are hindered by the difficulty of knowing, and controlling, the location of biomolecules within silica: the distribution of biomolecule structures and adsorption states present within biosilicas prevents clear quantitative characterisation,[26] necessitating the use of model systems.[27] Recently we developed a method of post-synthetically modifying BIS materials to control the elution of some or all of the additive molecule from within the composite material by changing acidity of a BIS suspension,[35] enabling investigation of silica surface chemistry after additive removal without surface dehydration associated with prior methods i.e. calcination. Notably, both the BIS synthesis technique and later elution produced consistent amounts of additive within the silica material, indicating that the amount of elution a function of the silica surface charge and therefore that the most loosely-held additives are eluted first. We believe that this unprecedented control over the silica-organic interface can be a powerful tool to help characterise interfacial interactions in hybrid silica materials.

In this study, we combined the previously-developed acid elution technique with solid-state NMR experiments probing ^{1}H and ^{29}Si to resolve the local structure and surface chemistry of this BIS at different levels of activation (i.e. PEHA removal), assessing how surface bonding is affected by PEHA's initial incorporation and subsequent removal. By comparing this against amine-free industrially precipitated silica (IPS) and IPS, which has been exposed to PEHA, we show the lasting impact PEHA has on silica polymerisation and how this may relate to other nanocomposite silica materials.

Experimental

Silica synthesis and modification

Silica was synthesised according to methods previously published by the authors.[35,38] Briefly, solutions of sodium silicate pentahydrate (*Fisher Scientific, technical grade*) and pentaethylenehexamine (*Sigma Aldrich, technical grade*) were separately prepared corresponding to final reaction concentrations of 30

mM each of Si and N. These were then mixed, neutralised in a single step using 1M HCl (*Fisher scientific, stabilised*), and allowed to react for 5 minutes under stirring.

After 5 minutes, further 1M HCl was added to the silica coagulum to reduce the pH from 7 to either 5 or 2. After the pH had subsequently stabilised (ca. 1 minute unless otherwise noted), the materials were isolated by centrifugation at 5000*g* for 15 minutes. The supernatant was then decanted, and this centrifugation procedure repeated twice using deionised water to wash the samples of any salts and unreacted reagents. After the last wash, the supernatant was decanted, and the silica allowed to dry in an oven at 80 ^{o}C overnight.

For the industrial precipitated silica samples, 100 mg of pre-made silica (*Grace, Syloid AL-1 FP grade*) was suspended in 100 mL deionised water. The samples were titrated using 1M HCl and 2M NaOH (prepared from sodium hydroxide pellets, *Fisher Scientific, analytical grade*) to the same pH as for the bioinspired silica materials. Due to the low initial electrolyte concentration, the pH was allowed to equilibrate overnight before separation, washing and drying as described above.

Premade IPS was also exposed to PEHA to assess any impact the additive has on the surface chemistry of pre-made silica. This was performed at two concentrations; one in which the additive concentration was approximately equal to that used in the BIS synthesis procedure, and one in which the additive concentration was significantly higher. For the lower concentration, 100 mg of IPS was added to 95 mL 5 mM PEHA solution (corresponding to 30 mM dissolved nitrogen, as before). This suspension was then neutralised with 1 N H_2SO_4, and the final volume made up to 100 mL. The higher concentration was prepared by suspending 100 mg IPS in 0.5 ml 250 mM PEHA solution, which was then neutralised as before and made up to a total volume of 2 mL. Solutions were agitated for 1 hour using magnetic stirrer bars before being left to stand for a further 18 hours at ambient temperature (ca. 20 ^{o}C), and isolated as described for BIS. For comparison, as made BIS samples containing PEHA were also aged overnight and CHN experiments were performed on these "aged-BIS" samples as described previously (see ref 35).

Solid state NMR experiments

Solid state single pulse ^{29}Si MAS NMR and ^{1}H-^{29}Si CP MAS NMR spectra were acquired on a Bruker Avance III HD 500 spectrometer at 11.7 T (B_0) using a 4.0mm dual resonance CP/MAS probe, yielding a Larmor frequency of 99.35 MHz. ^{29}Si MAS NMR spectra were acquired using a 4 μs non-selective ($\pi/2$) excitation pulse, a measured 90 s relaxation delay, a total of 256 scans and spinning at 12.5 kHz. ^{1}H-^{29}Si cross-polarisation (CP) MAS NMR experiments were performed using the same instrument with a spinning frequency of 12.5 kHz, a ^{29}Si non-selective ($\pi/2$) pulse width of 4.0 μs, an initial ^{1}H non-selective ($\pi/2$) pulse width of 2.5 μs, a recycle delay of 3 s and Hartmann-Hahn contact periods of 2 ms. A nominal ^{1}H decoupling field strength of 80 kHz was employed during acquisition and 1456 scans were collected per experiment. ^{1}H MAS NMR spectra were acquired using a 2.5 μs non-selective ($\pi/2$) excitation pulse, a single scan and spinning at 12.5 kHz. All ^{29}Si spectra were referenced to tetramethylsilane (TMS) at 0 ppm and all ^{1}H spectra were referenced to liquid H_2O at 4.7 ppm. Gaussian peak profiles were used to deconvolute the ^{29}Si MAS NMR and ^{1}H-^{29}Si CP MAS NMR spectra.[39] The minimum possible number of peaks were fitted, and the chemical shift (δ_{iso}) and peak full width at half maximum (FWHM) of each resonance were required to be consistent in both the ^{29}Si MAS NMR and ^{1}H-^{29}Si CP MAS NMR spectra. When fitting the data δ_{iso} and FWHM were held constant for each site within the same sample (i.e. only peak intensity was allowed to vary). NMR parameters are for all spectra are shown in Tables S1, S2, S3, and S4 for BIS, aged BIS, IPS, and modified-IPS respectively.

Results and Discussion

^{29}Si MAS NMR

BIS was synthesised by room-temperature precipitation at pH 7 using PEHA as a bioinspired additive.[38] These, and samples of IPS, were acidified to change the surface charge and hence PEHA surface concentration in the case of BIS (see Supporting Information and ref.35 for details). Samples were therefore titrated to pH 7 (corresponding to as-made BIS), pH 5 (partial PEHA removal), and pH 2 (full PEHA removal). These were then analysed by ^{29}Si MAS NMR to study how PEHA removal affected the silica structure itself (Figure 1, below). ^{29}Si MAS NMR enables distinction between fully saturated silicon centres (Q^4 at ca. δ_{iso} = -110 ppm) with singly hydroxylated (Q^3, ca. δ_{iso} = -100 ppm) and doubly hydroxylated (Q^2, ca. δ_{iso} = -90 ppm) Si centres,[40] and hence quantification of their relative abundance

in the material. From this, the degree of polymerisation in BIS was observed to be higher than in industrial silica (Table 1). This is unexpected as polymerisation of silica from Q^3 to Q^4 is generally considered to occur through syneresis[41] – the slow condensation of silica to expel water from the framework – which should be more prevalent in the industrial silica material due to its significantly longer reaction times (2-3 hours vs 5 minutes)[12] and similar micron-scale aggregate sizes compared to BIS.[35,42]

Table 1 – Comparison of relative peak integral areas for silicon species within IPS and BIS materials against pH for both single-pulse ^{29}Si MAS NMR and ^{1}H-^{29}Si CP MAS NMR data. Error bars are one standard deviation around the mean (n=3 silica samples), rounded to the nearest integer.

Relative peak area (%)	pH 7- Precipitated		pH 7 - Bioinspired		pH 7 - Bioinspired (aged 24 hours)		pH 5 – Precipitated		pH 5 – Bioinspired		pH 2 - Precipitated		pH 2 - bioinspired	
	^{29}Si	^{1}H-^{29}Si	^{29}Si	^{1}H-^{29}Si	^{29}Si	^{1}H-^{29}Si	^{29}Si	^{1}H-^{29}Si	^{29}Si	^{1}H-^{29}Si	^{29}Si	^{1}H-^{29}Si	^{29}Si	^{1}H-^{29}Si
Q^2	6	14	7	12	4 ± 0	12 ± 1	8	20	5	8	9	20	5	13
Q^3	39	77	34	47	32 ± 1	65 ± 1	42	71	34	53	43	72	33	69
Q^4	55	9	59	41	64 ± 1	17 ± 1	50	9	61	39	48	9	62	18

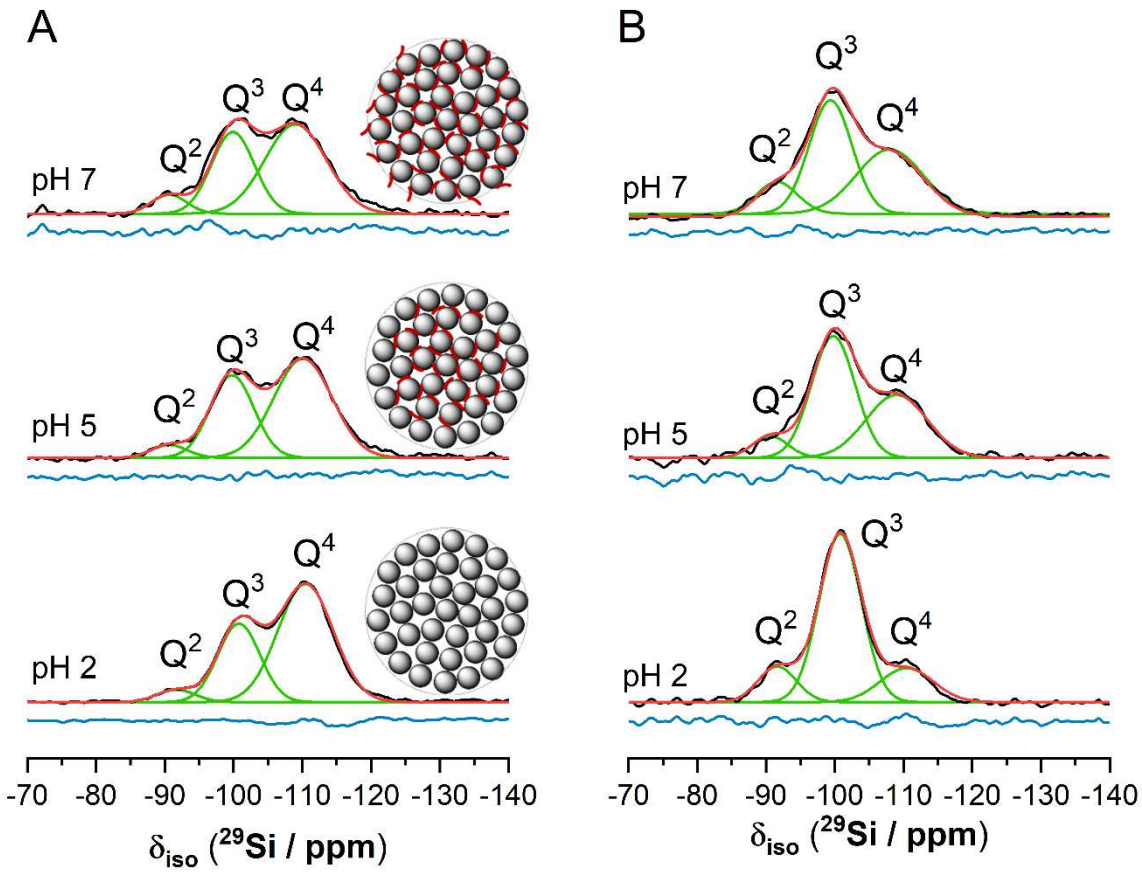

Figure 1 - ^{29}Si single-pulse MAS NMR spectra for (A) BIS and (B) IPS washed at pH 7 (top), 5 (middle), and 2 (bottom) and associated deconvolutions. Overlaid are representative schemes (adapted from ref. 31) of BIS: silica primary particles (grey circles) containing PEHA molecules (red lines) at as-made concentration (top), partially extracted (middle) and fully extracted (bottom). NMR spectra shown are the original data (black), individual resonance contributions (green), fitted sum of individual contributions (red), and residual (blue).

Upon modification of pH, the surface Si speciation of IPS changed slightly to include fewer Q^4 sites (from 55% relative abundance at pH 7 to 48% relative abundance at pH 2), and correspondingly more Q^3 and Q^2 sites (Figure 2). This is in good agreement with previous studies on the acid treatment of precipitated silicas, which found an increase in Q^3 relative abundance of up to 10% under similar conditions.[43] For BIS, such pH-based changes were not seen (Q^4 sites remained at approximately 60% relative abundance across all pH values).

PEHA has been shown to be effective at 'passivating' silica surfaces to prevent dissolution in undersaturated Si solutions.[44] Therefore, IPS modification with PEHA was attempted to observe its

effect on the surface chemistry of premade silica and determine if the difference in measured Q^n ratios resulted from the presence of PEHA in solution or was intrinsic to the BIS materials. To ensure direct comparison between modified IPS and BIS, further BIS samples were synthesised and aged at ca. pH 7 for a similar time (i.e. untreated for 24 hours) prior to isolation.

After exposing IPS to PEHA, the relative Q^4 concentration was again slightly lowered compared to the pH 7 sample (from 59% to 48% or 53% relative abundance at low and high [PEHA], respectively, see table S3), with concurrent increases in Q^3 and Q^2 prevalence. This runs counter to the stabilisation observed in the previous study, although the effect could be due to higher overall [Si] (ca. 30 mM herein, cf. 1 mM in reference [44]) or higher ionic strength during IPS modification (see Table S5). Regardless, it is clear that addition of PEHA to silica materials post-synthesis did not replicate the high and sustained condensation states observed in BIS. Similar behaviour was not exhibited during aging of BIS samples (Table S2), wherein Q^3 prevalence remained the same (32±1%, cf. 34% for unaged BIS), and Q^4 prevalence increased slightly at the expense of Q^2 species (64±1% and 4±0% cf. 59 and 7% for unaged BIS). Despite the increased silica condensation, aged BIS samples exhibited an unexpected decrease in PEHA content - from 0.64 mmol/g to 0.12 mmol/g (indicating a *ca.* 80% removal, see Table S6) - indicative of significant leaching of the additive.

Overall, the ^{29}Si MAS NMR data indicates that BIS was in fact more stable than IPS. This is significant because even after removal of the PEHA by elution to pH 2 or 24 hours of aging, BIS maintained a high Q^4 concentration, indicating that the structures have a higher hydrothermal stability even after purification.[45,46] This provides the first direct comparison of BIS hydrothermal stability against industrial silicas, showing that the use of bioinspired additives creates more stable materials.

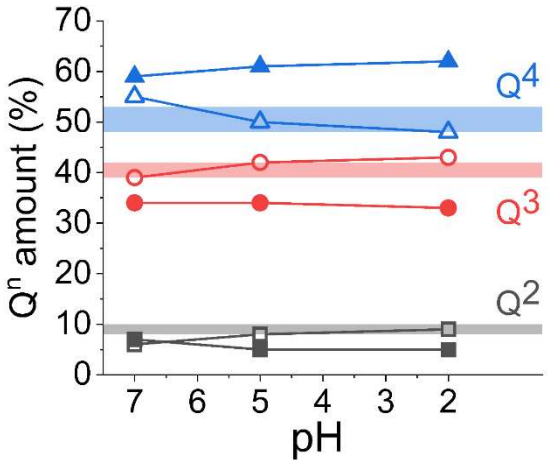

Figure 2 – Relative abundance of Si Q^n species (determined from the ^{29}Si single-pulse MAS NMR spectral deconvolutions) against extraction pH for IPS (open shapes) and BIS (filled) silica materials (with greater degree of extraction at lower pH). Overlaid bars are equivalent relative abundance for PEHA-modified IPS materials. Black squares represent Q^2 species, red circles represent Q^3 species, and blue triangles represent Q^4 species.

Given that BIS was found to be more condensed than IPS even after PEHA extraction/leaching, we hypothesise that the additive (PEHA) might be causing these effects during the initial synthesis. In order to test this hypothesis, we probed the interaction between silica and the adsorbed additive to determine the localisation of PEHA-surface interaction and why this causes lower susceptibility to attack by acidic medium even after full PEHA loss.

^{1}H MAS NMR

Initially, ^{1}H MAS NMR data for the three silica materials were gathered to observe any changes to the silanol chemical environment upon addition of PEHA. For IPS, a single well defined peak was observed at approximately δ_{iso} =5.5 ppm for all samples (Figure 3a), indicating a uniform chemical environment for the silanol species therein (corresponding to water molecules hydrogen-bonded to silanol groups).[47] Introduction of PEHA to IPS led to significant broadening of the ^{1}H MAS NMR resonance as well as peak shifting to higher ppm values (ca. δ_{iso} = 6.5 ppm, corresponding to previous reports of ammonium hydroxide in silica zeolites, Figure 3b).[48] Peak broadening was even more pronounced for as-made BIS (Figure 3c), indicating that PEHA encapsulated during synthesis led to a wider range of local Si chemical environments. Upon extraction of PEHA from BIS by lowering the pH the peak broadening

reduced until, at pH 2, a ^{1}H MAS NMR spectrum was observed that exhibited a line-shape similar to that of IPS.

This indicates that, although the quantity of Si-OH moieties was different between BIS and IPS at pH 2, the chemical environment in each of those moieties was similar. Furthermore, with regards to the goal of using acid elution of additives as a means of controlling organic localisation within a silica matrix, we note that PEHA-modified IPS appears qualitatively similar to BIS treated to pH 5, but not as-made (pH 7) BIS (Figure 3b and c, respectively). The emergence of more well-defined peaks after partial extraction agrees with the authors' earlier supposition that more loosely held additives are extracted first,[35] and therefore suggests that partial extraction can indeed be used as a tool to ensure uniform organic entrapment within a BIS matrix.

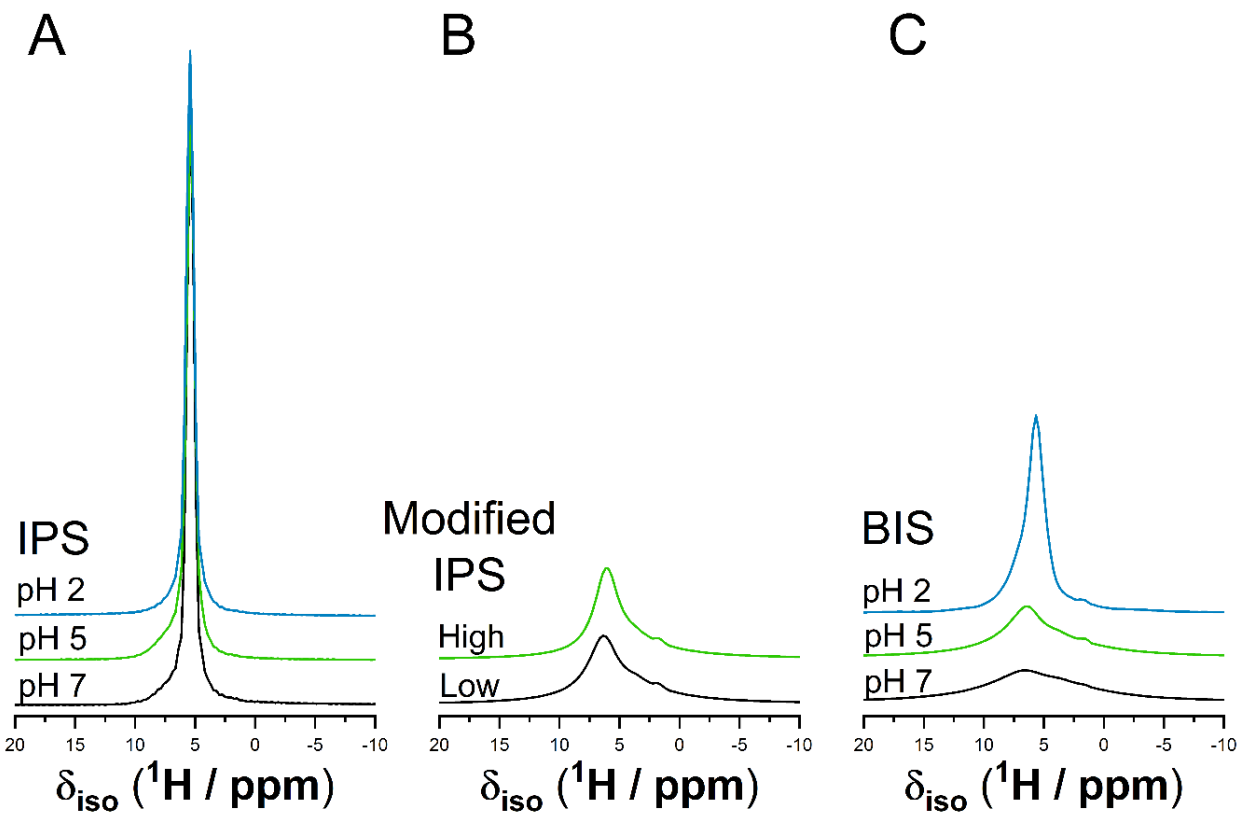

Figure 3 - ^{1}H MAS NMR spectra for (a) IPS at pH 7 (black), 5 (green), and 2 (blue), (b) PEHA-modified IPS at low (black) and high (green) PEHA concentration, and (c) BIS at pH 7 (black), 5 (green), and 2 (blue).

^{1}H-^{29}Si cross polarisation MAS NMR

Although both the ^{29}Si and ^{1}H MAS NMR data provide insight into the effect of PEHA on BIS chemistry, no specific details about the PEHA-silica binding were revealed. To better elucidate this, the bonding environment of Si with its proximate protons were measured using ^{1}H-^{29}Si CP MAS NMR. In the absence of any additives, we expect that Q^2 and Q^3 Si signals will be amplified as they are covalently connected to hydroxyl groups (hence protons), while Q^4 Si resonances will be dampened due to the absence of any protons within close proximity. Indeed, for the IPS, ^{1}H-^{29}Si CP MAS NMR data exhibited amplified Q^2 and Q^3 silica signals and suppressed Q^4 signals (Tables 1, S2 and Figure 4) regardless of the treatment pH. For BIS, ^{1}H-^{29}Si CP MAS NMR data showed significant differences for all pH treatments due to the presence (or absence) of PEHA (Figure 4). Compared to the IPS, BIS containing PEHA (pH 7 and pH 5) had relatively large Q^4 signals (ca. 40% cf. 9% in IPS) and smaller Q^3 and Q^2 signals in the ^{1}H-^{29}Si CP MAS NMR spectra (Figure 5). However, upon removal of PEHA (pH 2, or aging for 24 hours) this effect diminished and the relative amount of Q^2 and Q^3 signals increased, similar to that of their IPS counterparts. Interestingly, ^{1}H-^{29}Si CP MAS NMR data showed that the surface hydroxylation of PEHA-modified IPS differed from that of both unmodified IPS and BIS, with only minor suppression of the Q^3 signal to ca. 55% cf, 75% in IPS and ca. 47% in BIS (as well as concurrent Q^4 amplification, see Figure 5).

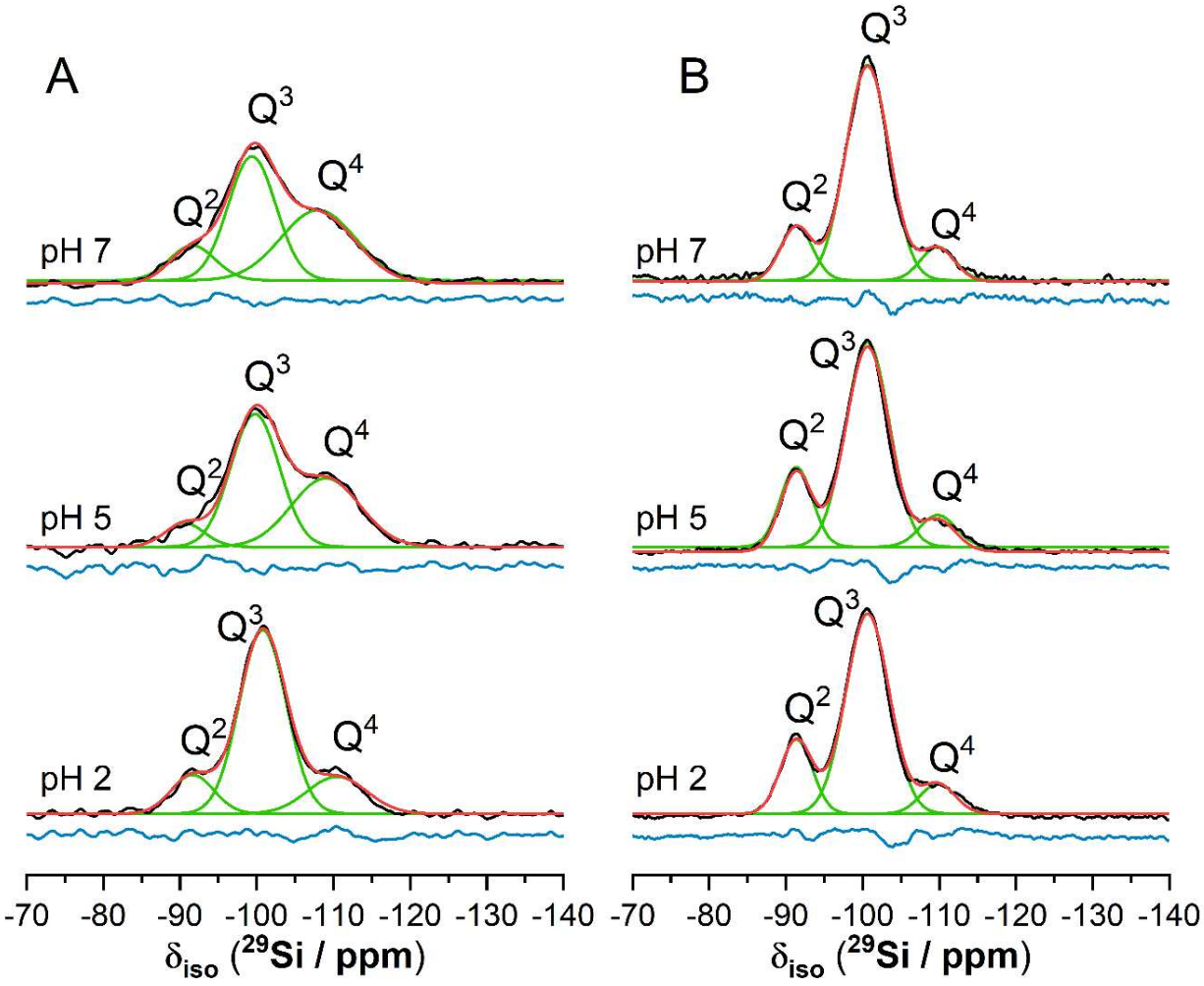

Figure 4 - ^{1}H-^{29}Si CP MAS NMR spectra for (A) BIS and (B) IPS washed at pH 7 (top), 5 (middle), and 2 (bottom) and associated deconvolutions. Shown are the original data (black), individual resonance contributions (green), fitted sum of individual contributions (red), and residual (blue).

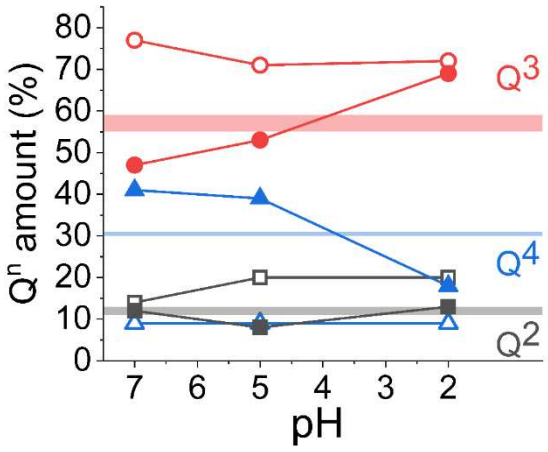

Figure 5 - Relative abundance of ^{1}H-proximate Si Q^n species (determined from the ^{1}H-^{29}Si CP MAS NMR spectra) against extraction pH for IPS (open shapes) and BIS (filled shapes) silica materials (with greater degree of extraction at lower pH). Overlaid bars are equivalent relative abundance for PEHA-modified IPS materials. Black squares represent Q^2 species, red circles represent Q^3 species, and blue triangles represent Q^4 species.

The ^{1}H-^{29}Si CP MAS NMR data suggest that, in addition to creating more Q^4 species in BIS, PEHA forms an adduct with Q^4 Si sites in general; Q^4 signals were enhanced in both BIS and modified IPS materials. This agrees with the results of Folliet et al, which proposed amine-Q^4 hydrogen bonding as part of quantum chemical simulations.[34] However, these findings appear to contradict previous simulation and experimental results for artificial templated silica systems, which show electrostatic or ion-pairing interactions only during surface adsorption of PEHA (or other amine molecules) i.e. onto deprotonated Q^3 Si centres only.[27,35,49,50] Previous studies of dried silica surfaces have shown secondary interactions with surrounding moieties are possible,[26] therefore PEHA-Q^4 adducts may be the result of secondary interactions on (partially) dried BIS surfaces.

However, this explanation for the detected ^{1}H-Q^4 adducts cannot explain why the absolute Q^4 concentration is enhanced in BIS materials compared to either IPS or modified-IPS materials. To explain this, we first note that PEHA has been shown to act as a catalyst in the initial condensation of silicic acid monomers, presumably through proton transfer. This was previously assumed to occur only in the solution-phase during synthesis,[49,51] where PEHA can freely disassociate from any silicate centre after condensation due to weaker interaction with the now covalently-saturated oxygen atom. Based on our findings, we posit that this catalysis continues after the amine molecule is physically trapped within the silica matrix (analogous to the "embedded" state recently proposed by Montagna et al.[27]). In this

case, desorption of PEHA after the Q^3 sites have been polymerised is hindered, leading to and the higher initial ^1H-Q^4 adduct concentration, which disappears after 24 hours.

The varying representation of surface additive-silica reactivity are visualised in Figure 6. In the absence of additives, silica condensation is known to occur through charged SiO^- moieties nucleophically attacking Si-OH centres, eventually leading to elimination of OH- (A); given the reported pKa of 6.8, these moieties are approximately equally abundant at pH 7.[52,53] Prior MD results indicate that PEHA attaches to such SiO^- surface sites during silica synthesis (B), and that the SiO^- density is sufficiently low that PEHA can only 'see' one such site. This predisposes us to think that further surface condensation only leads to PEHA dissociation (C) and presumably re-association at a different Q^3 site. The results we have found, combined with the recently published report by Montagna et al.,[27] indicate this is not the case. Instead, PEHA interacts with multiple surface sites, facilitated by the embedded configuration (D). These SiO^- moieties then polymerise further (E), leading to the unexpected PEHA-Q^4 adducts seen in unaged BIS samples. PEHA then slowly leaches away from the surface, bringing the CP MAS results in line with modified IPS while retaining the highly condensed surface chemistry.

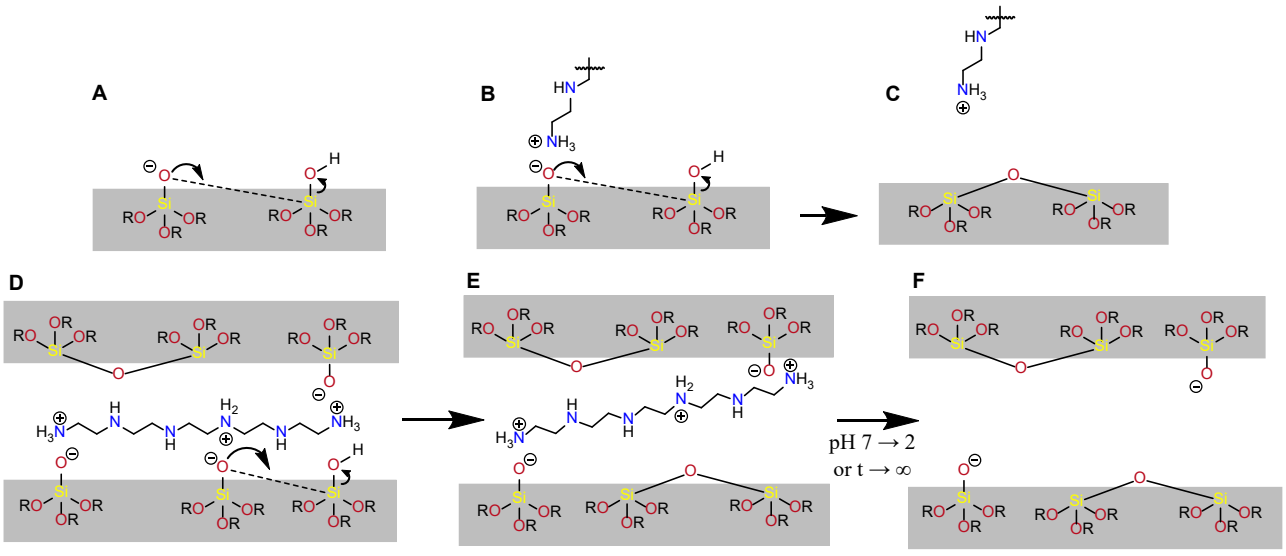

Figure 6 - Scheme visualising potential mechanisms of surface silanol condensation of BIS materials at pH 7. (A) In the absence of organic additives, (B-C) At single silica surfaces, wherein the additive can feely desorb after elimination of surface SiO^- moiety, and (D-E) in the "embedded" state, wherein additives remain in close contact with the surface after polymerisation of some surface SiO^- moieties, before slowly leaching from the material. OH^- leaving groups are omitted in each case for clarity.

These findings continue a pattern where higher condensation is associated with multifunctional additives only (either biopolymers or artificial compounds).[25] Q^4-template adducts have previously been detected in the cell walls of the diatom *Thalassiosira pseudonana*[28] as well as oligo-[33] and monopeptides[32] derived from the proteins therein. However, since the vast majority of artificially-templated silica materials use monofunctional templates which would be unable to make secondary interactions of these kinds with their silica surfaces, we conclude that polyfunctionality appears to be the key factor in determining if template-Q^4 interactions can occur.

Accordingly, these results provide a useful indication of how template functionality may be employed to tailor surface chemistry. By taking advantage of polyfunctional (and especially catalytically-active) additive compounds, artificially-templated silicas with higher degrees of surface condensation and hence hydrothermal stability could be designed without recourse to post-synthetic functionalisation or changes to the material recipe itself – a key challenge in current templated silica design.[54] With regards to biosilica materials, this finding can provide a tentative explanation on a molecular level for complex and hard-to-analyse biological phenomena such as bio-sintering – the fusing of silica lamella in the core of sponge spicules.[55] This process has been theorised to occur through continued catalytic activity of silica-depositing proteins trapped within already-formed sponge spicules.[56] Our findings suggest a potential route to direct investigation of bio-sintering by highlighting the similarities of BIS materials made with different polyfunctional additives and biosilica, and also by showing how use of BIS enables investigation through modification of the material post-synthetically while preserving the silica surface chemistry.. Furthermore, this indicates that BIS materials may be useful as model systems to study biosilica formation. Given the range of different bioinspired template structures,[57] specific biological motifs or even general physical properties can be replicated and studied in isolation, providing a reductionist insight into the more complex biological systems.

Finally, we believe our results highlight a potentially important difference between current atomistic and ab-initio simulations of silica surfaces. Our findings indicate that additive-Q^4 interactions, which have been positively identified during quantum chemical simulations but not in forcefield based methods, are more prevalent than previously considered and therefore current atomistic simulations of

solvated silica are not enough to fully describe the interfacial chemistry. Further, simulations on partially or fully dewatered surfaces (such as those reported in reference [26] are needed to fully describe the more complex interfacial chemistry present in systems with polyfunctional templates. Future research focusing on solid state NMR experiments directly probing ^{13}C and ^{15}N nuclei on isotopically labelled PEHA and other bioinspired additives, as well as experiments probing ^{13}C-^{29}Si and ^{15}N-^{29}Si internuclear distances (e.g. ^{13}C-^{29}Si and ^{15}N-^{29}Si CP, HETCOR, or REDOR MAS NMR) will be vital to further resolve the surface PEHA-silica interactions and PEHA-mediated silica synthesis.

Summary and Conclusions

Bioinspired silica materials were produced using the additive PEHA and analysed by solid state ^{1}H MAS, ^{29}Si MAS and ^{1}H-^{29}Si CP MAS NMR after treatment to a range of different pH values. These were then compared against industrial precipitated silica (both treated to equivalent pH levels and after modification with PEHA), finding significantly higher condensation in the BIS despite having a lower reaction time, even after modification with the catalytic PEHA template. This signifies that bioinspired synthesis methods can produce more hydrothermally stable silica than current industrial practises, a key property for the materials.

^{1}H-^{29}Si CP MAS data showed that the additional Q^4 sites associate with the PEHA additive, a phenomenon which has only been previously observed in biomolecule- or polymer-templated silica materials. We propose that these adducts arise due to secondary additive-silica interactions from organic additives in the "embedded" configuration, something which is impossible for more commonly-studied monofunctional templates. These results highlight that BIS lies at the intersection between biosilica and artificially-templated silica materials, providing the advantages of catalytically-active templating behaviour to artificially-templated silica materials while enabling systematic investigation into the more complex interfacial phenomena present in biosilicas.

Separately, our investigations of aged BIS materials shows for the first time that the composition of bioinspired silicas is not constant over time. The loss of additives from within the silica-amine composite over a 24 hour period are highly surprising, especially given the author's pervious

demonstration of highly consistent silica compositions after a range of post-synthetic modification. This therefore necessitates further investigation of the kinetic stability of additive occlusion within BIS materials as a function of additive structure, solution composition, and synthesis conditions.

Overall, these findings are significant as they demonstrate an as-yet unexploited design space for artificially-templated silica materials, wherein the use of catalytically-active additives can be used to stabilise silica surfaces, even after their removal. Finally, this mechanism of surface cataltysis by embedded additive compounds provides a potential explanation for the biological phenomenon of bio-sintering in sponge spicules, and highlights overlooked details in current atomistic simulations of templated silica interfaces which are incapable of predicting such reactions.

Acknowledgements

We thank the EPSRC SynBIM project (EP/P006892/1), EPSRC Fellowship (EP/R025983/1), and ERC GROWMOF project (Prof. Tina Düren, ERC grant No. 648283) for their financial support. We thank the departments of Chemistry, Chemical and Biological Engineering, and Materials Science and Engineering at the University of Sheffield for funding and access to facilities. We thank Dr Sandra van Meurs for very insightful discussions and assistance with performing the NMR experiments. The authors declare no competing financial interests.

Supporting information

Tables of NMR peak deconvolution and relative integral area for all samples analysed. Graphs of ^{29}Si MAS and ^{1}H-^{29}Si CP MAS NMR spectra of modified IPS and aged BIS samples (including peak deconvolutions). Table of ionic strength for BIS and IPS samples prepared at different pH conditions. Table of CHN elemental analysis for Aged BIs samples.

References

(1) Duer, M. J. The Contribution of Solid-State NMR Spectroscopy to Understanding Biomineralization: Atomic and Molecular Structure of Bone. *J. Magn. Reson.* **2015**, *253*, 98–110.

(2) Hildebrand, M. Diatoms, Biomineralization Processes, and Genomics. *Chem. Rev.* **2008**, *108* (11), 4855–4874.

(3) Sumper, M.; Kröger, N. Silica Formation in Diatoms: The Function of Long-Chain Polyamines and Silaffins. *J. Mater. Chem.* **2004**, *14* (14), 2059–2065.

(4) Staniland, S. S.; Rawlings, A. E. Crystallizing the Function of the Magnetosome Membrane Mineralization Protein Mms6. *Biochem. Soc. Trans.* **2016**, *44* (3), 883–890.

(5) Dickerson, M. B.; Sandhage, K. H.; Naik, R. R. Protein- and Peptide-Directed Syntheses of Inorganic Materials. *Chem. Rev.* **2008**, *108* (11), 4935–4978.

(6) Patwardhan, S. V.; Patwardhan, G.; Perry, C. C. Interactions of Biomolecules with Inorganic Materials: Principles, Applications and Future Prospects. *J. Mater. Chem.* **2007**, *17* (28), 2875–2884.

(7) Coppage, R.; Slocik, J. M.; Sethi, M.; Pacardo, D. B.; Naik, R. R.; Knecht, M. R. Elucidation of Peptide Effects That Control the Activity of Nanoparticles. *Angew. Chemie Int. Ed.* **2010**, *49* (22), 3767–3770.

(8) Dang, X.; Yi, H.; Ham, M.-H.; Qi, J.; Yun, D. S.; Ladewski, R.; Strano, M. S.; Hammond, P. T.; Belcher, A. M. Virus-Templated Self-Assembled Single-Walled Carbon Nanotubes for Highly Efficient Electron Collection in Photovoltaic Devices. *Nat. Nanotechnol.* **2011**, *6* (6), 377–384.

(9) Grand View Research. *Specialty Silica Market Size, Share & Trend Analysis Report by Product*; 2018.

(10) Beck, J. S.; Vartuli, J. C.; Roth, W. J.; Leonowicz, M. E.; Kresge, C. T.; Schmitt, K. D.; Chu, C. T. W.; Olson, D. H.; Sheppard, E. W. A New Family of Mesoporous Molecular Sieves Prepared with Liquid Crystal Templates. *J. Am. Chem. Soc.* **1992**, *114* (27), 10834–10843.

(11) Gérardin, C.; Reboul, J.; Bonne, M.; Lebeau, B. Ecodesign of Ordered Mesoporous Silica Materials. *Chem. Soc. Rev.* **2013**, *42* (9), 4217–4255.

(12) Drummond, C.; McCann, R.; Patwardhan, S. V. A Feasibility Study of the Biologically Inspired Green Manufacturing of Precipitated Silica. *Chem. Eng. J.* **2014**, *244*, 483–492.

(13) Belton, D. J.; Patwardhan, S. V.; Annenkov, V. V.; Danilovtseva, E. N.; Perry, C. C. From Biosilicification to Tailored Materials: Optimizing Hydrophobic Domains and Resistance to Protonation of Polyamines. *Proc. Natl. Acad. Sci. U. S. A.* **2008**, *105* (16), 5963–5968.

(14) Jantschke, A.; Spinde, K.; Brunner, E. Electrostatic Interplay: The Interaction Triangle of Polyamines, Silicic Acid, and Phosphate Studied through Turbidity Measurements, Silicomolybdic Acid Test, and (29)Si NMR Spectroscopy. *Beilstein J. Nanotechnol.* **2014**, *5*, 2026–2035.

(15) Robinson, D. B.; Rognlien, J. L.; Bauer, C. A.; Simmons, B. A. Dependence of Amine-Accelerated Silicate Condensation on Amine Structure. *J. Mater. Chem.* **2007**, *17* (20), 2113.

(16) Babonneau, F.; Baccile, N.; Laurent, G.; Maquet, J.; Azaïs, T.; Gervais, C.; Bonhomme, C. Solid-State

Nuclear Magnetic Resonance: A Valuable Tool to Explore Organic-Inorganic Interfaces in Silica-Based Hybrid Materials. *Comptes Rendus Chim.* **2010**, *13* (1–2), 58–68.

(17) Rimola, A.; Costa, D.; Sodupe, M.; Lambert, J.-F. F.; Ugliengo, P. Silica Surface Features and Their Role in the Adsorption of Biomolecules: Computational Modeling and Experiments. *Chem. Rev.* **2013**, *113* (6), 4216–4313.

(18) Ravera, E.; Martelli, T.; Geiger, Y.; Fragai, M.; Goobes, G.; Luchinat, C. Biosilica and Bioinspired Silica Studied by Solid-State NMR. *Coord. Chem. Rev.* **2016**, *327–328*, 110–122.

(19) Emami, F. S.; Puddu, V.; Berry, R. J.; Varshney, V.; Patwardhan, S. V.; Perry, C. C.; Heinz, H. Prediction of Specific Biomolecule Adsorption on Silica Surfaces as a Function of PH and Particle Size. *Chem. Mater.* **2014**, *26* (19), 5725–5734.

(20) Heinz, H.; Pramanik, C.; Heinz, O.; Ding, Y.; Mishra, R. K.; Marchon, D.; Flatt, R. J.; Estrela-Lopis, I.; Llop, J.; Moya, S.; et al. Nanoparticle Decoration with Surfactants: Molecular Interactions, Assembly, and Applications. *Surf. Sci. Rep.* **2017**, *72* (1), 1–58.

(21) Jorge, M.; Milne, A. W.; Sobek, O. N.; Centi, A.; Pérez-Sánchez, G.; Gomes, J. R. B. B. Modelling the Self-Assembly of Silica-Based Mesoporous Materials. *Mol. Simul.* **2018**, *44* (6), 435–452.

(22) Baccile, N.; Laurent, G.; Bonhomme, C.; Innocenzi, P.; Babonneau, F. Solid-State NMR Characterization of the Surfactant−silica Interface in Templated Silicas: Acidic versus Basic Conditions. *Chem. Mater.* **2007**, *19* (6), 1343–1354.

(23) Tanev, P. T.; Pinnavaia, T. J. Mesoporous Silica Molecular Sieves Prepared by Ionic and Neutral Surfactant Templating: A Comparison of Physical Properties. *Chem. Mater.* **1996**, *8* (8), 2068–2079.

(24) Centi, A.; Manning, J. R. H.; Srivastava, V.; Van Meurs, S.; Patwardhan, S. V.; Jorge, M. The Role of Charge-Matching in Nanoporous Materials Formation. *Mater. Horizons* **2019**, *6* (5), 1027–1033.

(25) Spinde, K.; Pachis, K.; Antonakaki, I.; Paasch, S.; Brunner, E.; Demadis, K. D. Influence of Polyamines and Related Macromolecules on Silicic Acid Polycondensation: Relevance to “Soluble Silicon Pools”? *Chem. Mater.* **2011**, *23* (21), 4676–4687.

(26) Brückner, S. I.; Donets, S.; Dianat, A.; Bobeth, M.; Gutiérrez, R.; Cuniberti, G.; Brunner, E. Probing Silica-Biomolecule Interactions by Solid-State NMR and Molecular Dynamics Simulations. *Langmuir* **2016**, *32* (44), 11698–11705.

(27) Montagna, M.; Brückner, S. I.; Dianat, A.; Gutierrez, R.; Daus, F.; Geyer, A.; Brunner, E.; Cuniberti, G. Interactions of Long-Chain Polyamines with Silica Studied by Molecular Dynamics Simulations and

Solid-State NMR Spectroscopy. *Langmuir* **2020**, *36* (39), 11600–11609.

(28) Wisser, D.; Brückner, S. I.; Wisser, F. M.; Althoff-Ospelt, G.; Getzschmann, J.; Kaskel, S.; Brunner, E. 1H-13C-29Si Triple Resonance and REDOR Solid-State NMR - A Tool to Study Interactions between Biosilica and Organic Molecules in Diatom Cell Walls. *Solid State Nucl. Magn. Reson.* **2015**, *66*, 33–39.

(29) Lutz, H.; Jaeger, V.; Schmüser, L.; Bonn, M.; Pfaendtner, J.; Weidner, T. The Structure of the Diatom Silaffin Peptide R5 within Freestanding Two-Dimensional Biosilica Sheets. *Angew. Chemie - Int. Ed.* **2017**, *56* (28), 8277–8280.

(30) Roehrich, A.; Drobny, G. Solid-State NMR Studies of Biomineralization Peptides and Proteins. *Acc. Chem. Res.* **2013**, *46* (9), 2136–2144.

(31) Abacilar, M.; Daus, F.; Haas, C.; Brückner, S. I.; Brunner, E.; Geyer, A. Synthesis and NMR Analysis of 13 C and 15 N-Labeled Long-Chain Polyamines (LCPAs). *RSC Adv.* **2016**, *6* (96), 93343–93348.

(32) Ben Shir, I.; Kababya, S.; Schmidt, A. Binding Specificity of Amino Acids to Amorphous Silica Surfaces: Solid-State NMR of Glycine on SBA-15. *J. Phys. Chem. C* **2012**, *116* (17), 9691–9702.

(33) Geiger, Y.; Gottlieb, H. E.; Akbey, Ü.; Oschkinat, H.; Goobes, G. Studying the Conformation of a Silaffin-Derived Pentalysine Peptide Embedded in Bioinspired Silica Using Solution and Dynamic Nuclear Polarization Magic-Angle Spinning NMR. *J. Am. Chem. Soc.* **2016**, *138* (17), 5561–5567.

(34) Folliet, N.; Gervais, C.; Costa, D.; Laurent, G.; Babonneau, F.; Stievano, L.; Lambert, J. F.; Tielens, F. A Molecular Picture of the Adsorption of Glycine in Mesoporous Silica through NMR Experiments Combined with DFT-D Calculations. *J. Phys. Chem. C* **2013**, *117* (8), 4104–4114.

(35) Manning, J. R. H.; Yip, T. W. S.; Centi, A.; Jorge, M.; Patwardhan, S. V. An Eco-Friendly, Tunable and Scalable Method for Producing Porous Functional Nanomaterials Designed Using Molecular Interactions. *ChemSusChem* **2017**, *10* (8), 1683–1691.

(36) Heinz, H. Clay Minerals for Nanocomposites and Biotechnology: Surface Modification, Dynamics and Responses to Stimuli. *Clay Miner.* **2012**, *47* (2), 205–230.

(37) Heinz, H.; Vaia, R. A.; Krishnamoorti, R.; Farmer, B. L. Self-Assembly of Alkylammonium Chains on Montmorillonite: Effect of Chain Length, Head Group Structure, and Cation Exchange Capacity. *Chem. Mater.* **2007**, *19* (1), 59–68.

(38) Manning, J. R. H.; Routoula, E.; Patwardhan, S. V. Preparation of Functional Silica Using a Bioinspired Method. *J. Vis. Exp.* **2018**, No. 138, 1–9.

(39) Massiot, D.; Fayon, F.; Capron, M.; King, I.; Le Calvé, S.; Alonso, B.; Durand, J.-O.; Bujoli, B.; Gan,

Z.; Hoatson, G. Modelling One- and Two-Dimensional Solid-State NMR Spectra. *Magn. Reson. Chem.* **2002**, *40* (1), 70–76.

(40) Engelhardt, G.; Michel, D. High-Resolution Solid-State NMR of Silicates and Zeolites; Wiley: Chichester, 1987; pp 147–149.

(41) Muñoz-Aguado, M. J.; Gregorkiewitz, M. Sol-Gel Synthesis of Microporous Amorphous Silica from Purely Inorganic Precursors. *J. Colloid Interface Sci.* **1997**, *185* (2), 459–465.

(42) W.R. Grace & Company. *Silicas for the Food Industry*; Columbia, MD, USA, 2006.

(43) Unger, K. K.; Lork, K. D.; Pfleiderer, B.; Albert, K.; Bayer, E. Impact of Acidic/Hydrothermal Treatment on Pore Structural and Chromatographic Properties of Porous Silicas. I. The Conventional Approach. *J. Chromatogr. A* **1991**, *556* (1–2), 395–406.

(44) Patwardhan, S. V.; Tilburey, G. E.; Perry, C. C. Interactions of Amines with Silicon Species in Undersaturated Solutions Leads to Dissolution and/or Precipitation of Silica. *Langmuir* **2011**, *27* (24), 15135–15145.

(45) Chen, C.-Y.; Xiao, S.-Q.; Davis, M. E. Studies on Ordered Mesoporous Materials III. Comparison of MCM-41 to Mesoporous Materials Derived from Kanemite. *Microporous Mater.* **1995**, *4* (1), 1–20.

(46) Iler, R. K. The Chemistry of Silica: Solubility, Polymerization, Colloid and Surface Properties, and Biochemistry; A Wiley-Interscience publication; Wiley, 1979; p 40.

(47) Grünberg, B.; Emmler, T.; Gedat, E.; Shenderovich, I.; Findenegg, G. H.; Limbach, H. H.; Buntkowsky, G. Hydrogen Bonding of Water Confined in Mesoporous Silica MCM-41 and SBA-15 Studied by 1H Solid-State NMR. *Chem. - A Eur. J.* **2004**, *10* (22), 5689–5696.

(48) Van Aelst, J.; Haouas, M.; Gobechiya, E.; Houthoofd, K.; Philippaerts, A.; Sree, S. P.; Kirschhock, C. E. A.; Jacobs, P.; Martens, J. A.; Sels, B. F.; et al. Hierarchization of USY Zeolite by NH4OH. A Postsynthetic Process Investigated by NMR and XRD. *J. Phys. Chem. C* **2014**, *118* (39), 22573–22582.

(49) Belton, D. J.; Patwardhan, S. V.; Perry, C. C. Spermine, Spermidine and Their Analogues Generate Tailored Silicas. *J. Mater. Chem.* **2005**, *15* (43), 4629.

(50) Patwardhan, S. V.; Emami, F. S.; Berry, R. J.; Jones, S. E.; Naik, R. R.; Deschaume, O.; Heinz, H.; Perry, C. C. Chemistry of Aqueous Silica Nanoparticle Surfaces and the Mechanism of Selective Peptide Adsorption. *J. Am. Chem. Soc.* **2012**, *134* (14), 6244–6256.

(51) Delak, K. M.; Sahai, N. Mechanisms of Amine-Catalyzed Organosilicate Hydrolysis at Circum-Neutral PH. *J. Phys. Chem. B* **2006**, *110* (36), 17819–17829.

(52) Belton, D. J.; Deschaume, O.; Perry, C. C. An Overview of the Fundamentals of the Chemistry of Silica with Relevance to Biosilicification and Technological Advances. *FEBS J.* **2012**, *279* (10), 1710–1720.

(53) Iler, R. K. The Chemistry of Silica: Solubility, Polymerization, Colloid and Surface Properties and Biochemistry of Silica; A Wiley-Interscience publication; Wiley, 1979; pp 182–185.

(54) Jiang, C.; Su, A.; Li, X.; Zhou, T.; He, D. Study on the Hydrothermal Stability of MCM-41 via Secondary Restructure. *Powder Technol.* **2012**, *221*, 371–374.

(55) Müller, W. E. G.; Wang, X.; Burghard, Z.; Bill, J.; Krasko, A.; Boreiko, A.; Schloßmacher, U.; Schröder, H. C.; Wiens, M. Bio-Sintering Processes in Hexactinellid Sponges: Fusion of Bio-Silica in Giant Basal Spicules from Monorhaphis Chuni. *J. Struct. Biol.* **2009**, *168* (3), 548–561.

(56) Wang, X.; Wiens, M.; Schloßmacher, U.; Jochum, K. P.; Schröder, H. C.; Müller, W. E. G. Bio-Sintering/Bio-Fusion of Silica in Sponge Spicules. *Adv. Eng. Mater.* **2012**, *14* (3), 4–12.

(57) Patwardhan, S. V. Biomimetic and Bioinspired Silica: Recent Developments and Applications. *Chem. Commun.* **2011**, *47* (27), 7567–7582.

TOC graphic

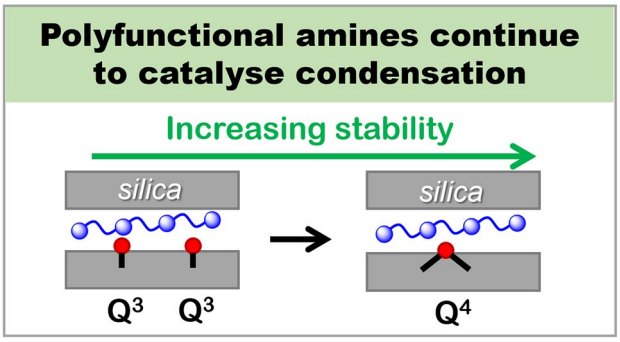
Polyfunctional amines continue to catalyse condensation
Increasing stability
silica
silica
Q3 Q3
Q4